ELSEVIER

Surface Science 429 (1999) L509–L514

surface science

www.elsevier.nl/locate/susc

Surface Science Letters

Asymmetric structure of the Si(111)-$\sqrt{3} \times \sqrt{3}$-Ag surface

H. Aizawa*, M. Tsukada, N. Sato, S. Hasegawa

Department of Physics, Graduate School of Science, University of Tokyo, 7-3-1, Hongo, Bunkyo-ku, Tokyo 113-0033, Japan

Received 26 February 1999; accepted for publication 17 March 1999

Abstract

The atomic and electronic structures of the Si(111)-$\sqrt{3} \times \sqrt{3}$-Ag surface are studied by first-principles calculations based on the density functional theory. It is found that a structural model consisting of two inequivalent Ag triangles is energetically more favorable than the well-established honeycomb-chained-triangle (HCT) model. The new structure should yield an empty-state STM image with a hexagonal-lattice pattern, rather than a honeycomb pattern, which is confirmed by low-temperature STM observations. © 1999 Elsevier Science B.V. All rights reserved.

Keywords: Density functional calculations; Metal–semiconductor interfaces; Scanning tunneling microscopy; Silicon; Silver; Surface relaxation and reconstruction

Although a great number of studies using a variety of experimental techniques to investigate surface structures were devoted to the Si(111)-$\sqrt{3} \times \sqrt{3}$-Ag surface, its atomic structure had been very controversial for a long time. For example, although two independent groups [1,2] obtained almost identical scanning tunneling microscopy (STM) images that exhibited a honeycomb pattern, the structural models they proposed are different from each other. One considered bright protrusions in the pattern to correspond to Ag atoms [1], the other to Si atoms [2]. Based upon their X-ray diffraction (XRD) data, however, Takahashi et al. proposed a model completely different from all the models that had been proposed before, which is now called the honeycomb-chained-triangle (HCT) model [3,4]. In this model, Ag adsorbates form chained triangles that are arranged in a honeycomb network, as shown in Fig. 1a. Though several experiments followed which supported this model (or models similar to it) [5–7], it appears inconsistent with the honeycomb STM pattern if one considers bright features in the pattern to represent the positions of the atoms in the top layer of the surface. Total energy calculations based on the density functional theory (DFT), however, clearly showed that the HCT model [4] has by far the lowest surface energy among all the proposed models [8]. Also, calculations of empty-state STM images for the HCT structure revealed that bright protrusions should lie at the centers of the Ag triangles, not at the positions of the Ag adsorbates [8,9]. Therefore, it

* Corresponding author. Present address: Department of Chemical Physics, Fritz-Haber-Institut der Max-Planck-Gesellschaft, Faradayweg 4–6, D14195 Berlin, Germany. Fax: +49-30-8413-4101.

E-mail address: aizawa@fhi-berlin.mpg.de (H. Aizawa)

0039-6028/99/$ – see front matter © 1999 Elsevier Science B.V. All rights reserved.
PII: S0039-6028(99)00424-0

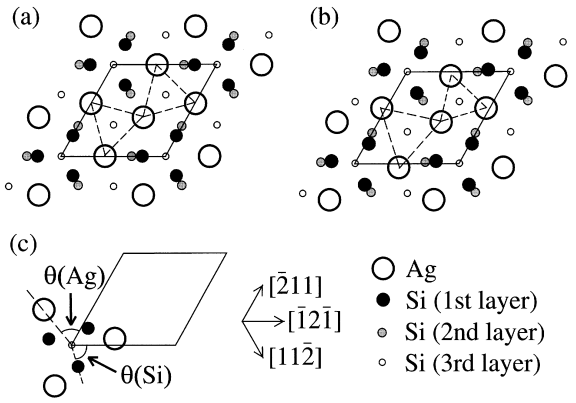

Fig. 1. Schematic illustrations of the (a) honeycomb-chained-triangle (HCT) and (b) inequivalent triangle (IET) models for the atomic structure of the Si(111)-$\sqrt{3}\times\sqrt{3}$-Ag surface. Solid lines indicate the unit cell, and dashed lines represent chained Ag triangles. In (c), the definitions of θ(Ag) and θ(Si) are illustrated.

now seems that there is almost no doubt that the HCT model is the only correct model for the atomic structure of the Si(111)-$\sqrt{3}\times\sqrt{3}$-Ag surface.

In this paper, however, we propose a new structural model, based on DFT total-energy calculations as well as low-temperature STM experiments. The new structure is calculated to be by 0.1 eV (per $\sqrt{3}\times\sqrt{3}$ unit cell) more stable than the HCT structure. Electronic band structures as well as charge density plots of a surface state are calculated for both structures, and several notable differences are pointed out. Especially, our calculations predict empty-state STM images with a hexagonal-lattice pattern instead of a honeycomb pattern for the new structure, which is verified by our STM observations.

The calculations were based upon the DFT with the local density approximation [10,11]. The Wigner-type exchange-correlation functional was used [12]. Wavefunctions were expanded by plane waves up to a cut-off energy of 40 Ry, and norm-conserving pseudopotentials [13,14] in the separable form [15] were employed. For Ag, 4d electrons as well as 5s electrons were treated explicitly. The pseudopotential for Ag used in the present calculation yields 4.16 Å for the lattice constant of the Ag crystal, in good accord with the experimental value of 4.09 Å. Nine uniform k-points were used to sample the Brillouin zone. We used a slab consisting of a silver layer, five silicon layers and a hydrogen layer terminating the bottom surface. The Si layers are composed of one single layer (upper) and two double layers (lower) with a missing top-layer configuration. The Ag layer as well as the upper three Si layers were allowed to relax in geometrical optimization procedures. The unit cell used has a periodicity of $(\sqrt{3}\times\sqrt{3})$R30°.

We first performed a geometrical optimization with the mirror-plane symmetry with respect to the [11$\bar{2}$] direction imposed, which resulted in the HCT structure (Fig. 1a). The top layer of the surface is composed of Ag triangles that are chained to each other, whereas the next layer consists of Si trimers. The optimized structural parameters are almost identical to those obtained by a previous calculation [8] except that the closest Ag–Si distance is slightly shorter in the present calculation (2.47 Å) than in the previous one (2.54 Å). This difference might be attributed to the use of different basis sets in the two calculations. In the previous calculation, a mixed basis set consisting of both LCAO-type basis functions and plane waves was used. In contrast, we used a basis set consisting only of plane waves. One of the advantages of a plane-wave basis set is that it is straightforward to check whether any results converge with respect to the basis set or not. We confirmed that all the important quantities (including the closest Si–Ag distance) did not vary when we increased the energy cut-off for the plane-wave basis set from 40 to 50 Ry.

The calculated electronic band structure is shown in Fig. 2a. The dispersive band around the Fermi level, called the S_1 band, is almost degenerate with (or crosses very slightly) the highest bulk valence band at $\boldsymbol{k}=\bar{\Gamma}$. This result is at variance with a calculation with LCAO-type expansions of wavefunctions, which shows a band gap of about 0.5 eV [9], but is in good agreement with a calculation using a mixed basis set [16]. Note that the S_1 band has been shown by a recent calculation to have bonding character with respect to the Si–Ag bonding at least at $\boldsymbol{k}=\bar{\Gamma}$ [17], although it had been believed to be an anti-bonding band. Besides

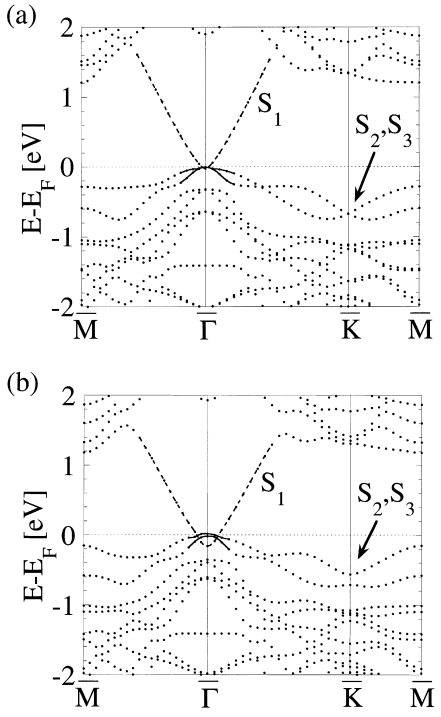

Fig. 2. Electronic band structures calculated for the (a) HCT and (b) IET models. The dashed lines represent the so-called S_1 surface-state bands, and the solid lines indicate the highest bulk valence bands.

the S_1 band, two other distinguished surface-state bands have been reported in the literature [18–20], called the S_2 and S_3 bands. Population analyses for the calculated wavefunctions have shown that the two states located around -0.6 eV (relative to the Fermi level) in the vicinity of $\boldsymbol{k}=\bar{\mathrm{K}}$ correspond to the S_2 and S_3 bands (so do the two states located around -0.3 eV in the vicinity of $\boldsymbol{k}=\bar{\Gamma}$). As is apparent from Fig. 2a, they are degenerate with each other at $\boldsymbol{k}=\bar{\mathrm{K}}$, which results from the fact that the HCT model has the mirror-plane symmetry with respect to the [11$\bar{2}$] direction. In fact, such degeneracy was suggested by an angle-resolved photoelectron spectroscopy (ARPES) study [18]. Fig. 3a displays a charge-density plot of the S_1 state with $\mathbf{k}=\bar{\Gamma}$. One can clearly see a honeycomb pattern, which is in accordance with previous STM results [1,2].

We then performed a geometrical optimization without any symmetry constraints. Surprisingly, it resulted in another structure (Fig. 1b) with a total energy 0.10 eV per unit cell lower than the HCT structure. As can be clearly seen by comparison between Fig. 1a and b, the two Ag triangles in the unit cell (indicated by dashed lines in Fig. 1) are of different sizes in the new structure, whereas they are of the same size in the HCT structure. The new structural model will be referred to hereafter as the inequivalent-triangle (IET) model. In contrast to the HCT model, the IET model has no mirror-plane symmetry with respect to the [11$\bar{2}$] direction. The two inequivalent Ag triangles are characterized by Ag–Ag distances of 3.00 and 3.89 Å, whereas the nearest Ag–Ag distance for the HCT structure is 3.44 Å. The Ag–Ag bonds with a length of 3.00 Å might be very strong, because they are close to the nearest-neighbor distance for the silver crystal (with the face-centered cubic structure), which is 2.89 Å. As is the case with the HCT structure, the IET structure also has the threefold rotational symmetry around an axis going through a Si atom in the third layer (e.g. each corner of the unit cell shown in Fig. 1). We present the values for several structural parameters for both the HCT and IET models in Table 1. Note that the Ag–Ag distance, d(Ag), and the orientation, θ(Ag), of the Ag triangle shown in Fig. 1c provides a complete description of the lateral positions of the atoms in the Ag layer, and that the same goes for the first Si layer. As can be seen from Table 1, the IET model is characterized by twistings of the Ag and Si triangles shown in Fig. 1c by 6° in the same direction as compared to the HCT model. Previously, Ichimiya et al. claimed that the Si trimers are twisted by about 20°, based on their reflection high-energy electron diffraction (RHEED) data, whereas there was no evidence of any twisting of the Ag triangles [6]. For the Si(111)-$\sqrt{3}\times\sqrt{3}$-Pd surface, it was suggested that the Pd trimers are twisted by 6°, though the Pd atoms are not considered to form chained triangles, in contrast to the case of Ag adsorption [21].

The band structure calculated for the IET model is presented in Fig. 2b. By comparison between Fig. 2a and b, one can see that the band structures for the HCT and IET models are rather similar. However, the degeneracy of the S_2 and S_3 surface

SURFACE SCIENCE LETTERS

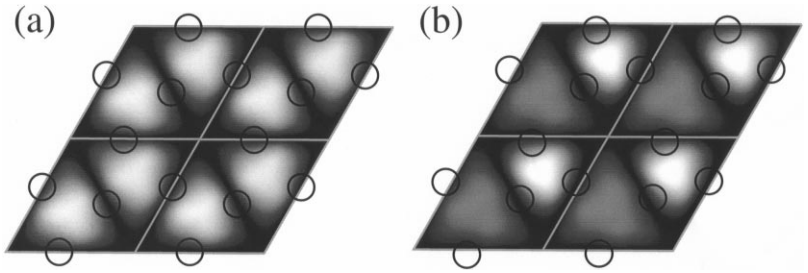

Fig. 3. Charge density plots of the S_1 state with $\boldsymbol{k}=\bar{\Gamma}$ at a plane parallel to the surface 1.7 Å above the Ag layer for the (a) HCT and (b) IET models. Bright and dark regions correspond to high and low charge densities, respectively, with different scales in each figure. The charge density at the brightest region in (b) is about 2.5 times as large as that at the brightest region in (a). Open circles represent the positions of Ag atoms, and gray lines indicate the unit cells.

states at $\boldsymbol{k}=\bar{\mathrm{K}}$ seen for the HCT structure is lifted for the IET structure, with the energy difference being 0.15 eV. It is also noted that the S_1 band, which crosses the highest bulk valence-band barely (by less than 0.01 eV) around $\mathbf{k}=\bar{\Gamma}$ for the HCT structure, crosses it more appreciably for the IET structure, the energy difference between the two bands at $\mathbf{k}=\bar{\Gamma}$ being 0.14 eV. Comparison of this feature to experiments might be difficult because band-bending effects cannot be rigorously incorporated into calculations.

A charge density plot of the S_1 state with $\mathbf{k}=\bar{\Gamma}$ is shown in Fig. 3b. It has been found that bright and dark features alternate with each other, corresponding to the small and large Ag triangles, respectively. The charge density at the center of the small triangle is about three times as large as that at the center of the large triangle. Thus, the IET structure is expected to yield empty-state STM images with a hexagonal-lattice pattern rather than a honeycomb pattern. Although we cannot discuss quantitatively the intensities of the bright and dark features in such STM images without performing elaborate tunneling-current calculations, as in Ref. [9], Fig. 3a and b suggest at least that STM measurements could very likely distinguish between the HCT and IET structures.

Table 1
Structural parameters calculated for the HCT (Fig. 1a) and IET (Fig. 1b) models of the Si(111)-$\sqrt{3}\times\sqrt{3}$-Ag surface[a]

Parameters	HCT	IET
θ(Ag) (°)	60	54
θ(Si) (°)	60	66
d(Ag) (Å)	4.88	4.88
d(Si) (Å)	2.55	2.58
z(Ag) (Å)	3.02	3.01
z(Si) (Å)	2.29	2.29

[a] For the definitions of θ(Ag) and θ(Si), see Fig. 1c. d(Ag) and d(Si) denote the Ag–Ag and Si–Si distances, respectively, for the atoms shown in Fig. 1c. z(Ag) and z(Si) denote the heights of the Ag and first Si layers, respectively, measured from the second Si layer.

In fact, such hexagonal-lattice images have been clearly observed by low-temperature STM. We used an ultra-high-vacuum, low-temperature STM equipped with a RHEED system for the preparation of sample surfaces. The base pressure in the chamber was less than 1×10^{-10} Torr. The substrate was an n-type Si(111) wafer with a resistivity of 0.005 Ω cm at room temperature, and an electrochemically etched polycrystalline W tip was used. The Si(111)-$\sqrt{3}\times\sqrt{3}$-Ag structure was prepared by depositing about 0.6 monolayer of Ag on the clean Si(111)-7×7 surface kept at 500°C. After this preparation, the sample was cooled down to 62 K on the STM stage.

Fig. 4a and b show empty-state STM images measured in the constant-current mode. Since the IET structure has no mirror-plane symmetry with respect to the [11$\bar{2}$] direction, there are two ways of twisting of the Ag and Si triangles, which can lead to two types of IET structure. Correspondingly, one can see two hexagonal-lattice patterns with different phases in the upper-right and lower-left parts of Fig. 4a. A honeycomb pattern is seen between them, which indicates that a region with the HCT structure exists between the two

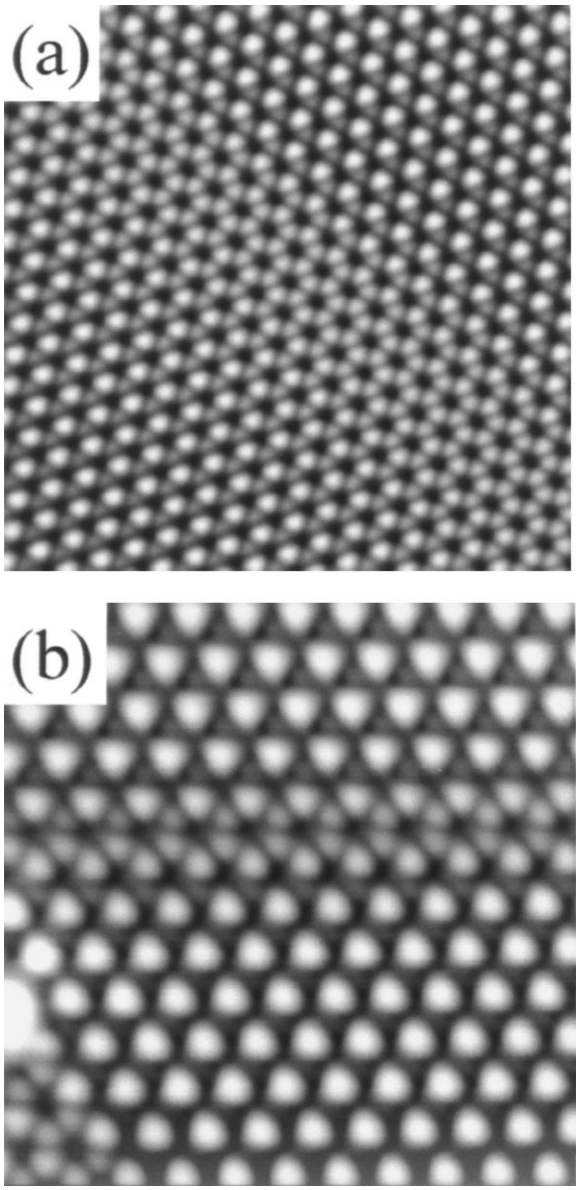

Fig. 4. Empty-state STM images measured at 62 K for two different regions of the Si(111)-$\sqrt{3}\times\sqrt{3}$-Ag surface. The displayed areas, tunneling currents, and sample bias voltages were (a) 115×115 Å^2, 1.3 nA, and 1.5 V, and (b) 80×80 Å^2, 1.0 nA, and 0.5 V.

types of IET structure. Fig. 4b also exhibits the two types of IET domain with a narrow HCT region as their domain boundary. Another HCT region can be seen around the lower left corner of Fig. 4b, which is adjacent to a 7×7 domain lying outside the displayed area. The HCT structure tends to appear only near such steps and at domain boundaries between the two types of IET structure at low temperature.

In conclusion, the DFT total-energy calculations have revealed a new structural model where a mirror-plane symmetry seen for the well-established HCT model is absent. The new model is expected to produce an empty-state STM image with a hexagonal-lattice pattern instead of a honeycomb pattern. Such an image has actually been observed in low-temperature STM experiments. It is anticipated that low-temperature measurements with other techniques such as ARPES and XRD will also confirm this structural model.

Acknowledgements

We wish to thank Prof. T. Takahashi, Prof. S. Watanabe, Prof. J. Yoshinobu, and Dr H. Nakatsuji for valuable discussions. We are grateful to Dr K. Kobayashi for pseudopotential data. This work has been supported in part by Grants-In-Aid for Creative Basic Research (No. 09NP1201) from the Ministry of Education, Science, Culture, and Sports of Japan, and also by CREST (Core Research for Evolutional Science and Technology) of the Japan Science and Technology Corporation.

References

[1] R.J. Wilson, S. Chiang, Phys. Rev. Lett. 58 (1987) 369.
[2] E.J. van Loenen, J.E. Demuth, R.M. Tromp, R.J. Hamers, Phys. Rev. Lett. 58 (1987) 373.
[3] T. Takahashi, S. Nakatani, N. Okamoto, T. Ishikawa, S. Kikuta, Jpn. J. Appl. Phys. 27 (1988) L753.
[4] T. Takahashi, S. Nakatani, N. Okamoto, T. Ishikawa, S. Kikuta, Surf. Sci. 242 (1991) 54.
[5] E. Vlieg, A.W. Denier van der Gon, J.F. van der Veen, J.E. Macdonald, C. Norris, Surf. Sci. 209 (1989) 100.
[6] A. Ichimiya, S. Kohmoto, T. Fujii, Y. Horio, Appl. Surf. Sci. 41–42 (1989) 82.
[7] M. Katayama, R.S. Williams, M. Kato, E. Nomura, M. Aono, Phys. Rev. Lett. 66 (1991) 2762.
[8] Y.G. Ding, C.T. Chan, K.M. Ho, Phys. Rev. Lett. 67 (1991) 1454.
[9] S. Watanabe, M. Aono, M. Tsukada, Phys. Rev. B 44 (1991) 8330.
[10] P. Hohenberg, W. Kohn, Phys. Rev. B 136 (1964) 864.

SURFACE SCIENCE LETTERS

[11] W. Kohn, L.J. Sham, Phys. Rev. A 140 (1965) 1133.
[12] E. Wigner, Phys. Rev. 46 (1934) 1002.
[13] G.B. Bachelet, D.R. Hamann, M. Schlüter, Phys. Rev. B 26 (1982) 4199.
[14] N. Troullier, J.L. Martins, Phys. Rev. B 43 (1991) 1993.
[15] L. Kleinman, D.M. Bylander, Phys. Rev. Lett. 48 (1982) 1425.
[16] Y.G. Ding, C.T. Chan, K.M. Ho, Phys. Rev. Lett. 69 (1992) 2452.
[17] H. Aizawa, M. Tsukada, Phys. Rev. B 59 (1999) 10923.
[18] L.S.O. Johansson, E. Landemark, C.J. Karlsson, R.I.G. Uhrberg, Phys. Rev. Lett. 63 (1989) 2092.
[19] S. Hasegawa, X. Tong, C.-S. Jiang, Y. Nakajima, T. Nagao, Surf. Sci. 386 (1997) 322.
[20] X. Tong, C.-S. Jiang, S. Hasegawa, Phys. Rev. B 57 (1998) 9015.
[21] K. Akiyama, K. Takayanagi, Y. Tanishiro, Surf. Sci. 205 (1988) 177.